


 Cite this: *RSC Adv.*, 2022, **12**, 19624

 Received 23rd May 2022
 Accepted 24th June 2022

 DOI: 10.1039/d2ra03230a
rsc.li/rsc-advances

Improvements in photoelectric performance of dye-sensitised solar cells using ionic liquid-modified TiO_2 electrodes†

 Tomohiko Inomata, ^a Ayaka Matsunaga, ^a Guangzhu Jin, ^a Takuma Kitagawa, ^a Mizuho Muramatsu, ^a Tomohiro Ozawa^a and Hideki Masuda ^{ab}

One of the major problems in dye-sensitised solar cells (DSSCs) is the aggregation of dyes on TiO_2 electrodes, which leads to undesirable electron transfer. Various anti-aggregation agents, such as deoxycholic acid, have been proposed and applied to prevent dye aggregation on the electrodes. In this study, we designed and synthesised a phosphonium-type ionic liquid that can be modified on the TiO_2 electrode surface and used as a new anti-aggregation agent. Although the modification of the ionic liquid onto the electrode reduced the amount of dye adsorbed on the electrode, it showed a significant anti-aggregation effect, thereby improving the photovoltaic performance of DSSCs with **N3** and **J13** dyes. This finding suggests that ionic liquids are effective as anti-aggregation agents for DSSCs.

Introduction

Dye-sensitised solar cells (DSSCs) are gaining attention as next-generation low-cost and energy-saving solar cells. As the manufacturing process of DSSCs does not require high vacuum or temperature, it is expected to consume less energy than that of conventional solar cells.^{1,2} In 1993, Grätzel *et al.* reported the **N3** dye, which is still widely used today because of its ability to absorb visible light up to 800 nm.³ The **N719** dye, in which two protons on **N3** are replaced by tetrabutylammonium ions (TBA^+), was reported in 1999;² its photoelectric conversion efficiency was as high as 11.2%.^{4,5} In addition, a conversion efficiency of 12.3% was achieved in a system using a DSSC that combined a zinc porphyrin complex (**YD2-o-C8**) with an organic dye (**Y123**), and a $\text{Co}^{2+}/\text{Co}^{3+}$ redox couple, $[\text{Co}(\text{bpy})_3]^{2+/3+}$.⁶ The **Z907** dye, in which the carboxyl group of one 4,4'-dicarboxy 2,2'-bipyridine (dcbpy) ligand on **N3** is replaced with a C_9H_{19} -group, has a photoelectric conversion efficiency of over 7%. It has been widely studied and is now recognised as a thermally stable dye.⁷⁻⁹

It is well known that one of the problems in DSSCs is the aggregation of dyes. The aggregation of dyes on the TiO_2 surface prevents the efficient conversion of absorbed light into electrical energy, and/or causes excited electrons to transfer to nearby dye oxidants. This is attributed to the low photovoltaic

performance of DSSCs. To improve the performance of DSSCs, various molecules have been explored and added to the dye solutions. For example, it was reported that the addition of cholic acid (CA) improved both the short-circuit current density (J_{SC}) and open-circuit voltage (V_{OC}) in a system containing porphyrin derivatives.¹⁰ Studies have also been conducted using hexadecylmalonic acid (HDMA),⁸ 1-decylphosphonic acid (DPA),⁷ 3-phenylpropionic acid (PPA),⁹ deoxycholic acid (DCA),¹¹ and chenodeoxycholic acid (CDCA).¹²⁻¹⁴ Among these, CDCA is the most common anti-aggregation agent. When the surface of TiO_2 is bare, reverse electron transfer can occur between the TiO_2 electrode and the electrolyte. While CDCA has been found to suppress reverse electron transfer, studies on the introduction of various blocking layers on the TiO_2 surfaces have also been conducted.¹⁵⁻¹⁷ In addition to the introduction of co-adsorbed molecules, it was reported that the stacking of metal oxides (such as SiO_2 , Al_2O_3 , and ZrO_2) on the TiO_2 surface suppressed electron recombination.¹⁸ It was also found that the adsorption of imidazolium-based insulator on the electrode surface prevented the aggregation of the dye and suppressed reverse electron transfer.¹⁹ Studies involving the use of different-sized siloxane molecules to cover the TiO_2 electrode surface have also been carried out.²⁰

An ionic liquid (**IL**) is a molten salt that generally maintains a liquid state below 100 °C. **ILs** have recently attracted attention as an environmentally friendly solvent.^{21,22} **ILs** are non-volatile and flame resistant. They have wide potential windows and low viscosity despite their ionic nature. Because of the non-volatility of **IL**, it can be recovered with almost high purity after being used in material production and can be reused. Moreover, **ILs** have been extensively studied as a green solvent owing to their excellent flame retardancy and stability. In the

^aDepartment of Life Science and Applied Chemistry, Graduate School of Science, Nagoya Institute of Technology, Gokiso-cho, Showa-ku, Nagoya 466-8555, Japan

^bDepartment of Applied Chemistry, Aichi Institute of Technology, 1247 Yachigusa, Yakusa-cho, Toyota 470-0392, Japan

† Electronic supplementary information (ESI) available. See <https://doi.org/10.1039/d2ra03230a>



21st century, ionic conductivity and thermal stability have attracted considerable attention. Therefore, **ILs** have been actively studied as electrolytes and reaction solvents for fuel cells,²³ DSSCs,^{24,25} and lithium-ion secondary batteries.²⁶ However, **ILs** are difficult to purify due to their low volatility, and their preparation is expensive. Therefore, the large-scale industrial application of **ILs** in batteries and cells is difficult.

Recently, our group reported a few studies on electrodes modified with bulky phosphonium/ammonium-type **ILs**. These include the capture of exogenous compounds,²⁷ four-electron reduction of molecular oxygen,²⁸ NO sensing in water,²⁹ and electrocatalytic CO₂ reduction.³⁰ The electrodes modified with bulky **ILs** provide a specific reaction field on the electrode surface that improves the stability and catalytic activity of the encapsulated compounds.

From the above-mentioned studies on **IL**-modified electrodes^{27–30} and the adsorption of the insulator which has the **IL**-like structure on the TiO₂ electrode,¹⁹ we decided to study the application of **ILs** as an anti-aggregation agent for DSSCs. Fig. 1 shows the schematic structures of the **ILs**, dyes, and the conventional anti-aggregation agent, **CDCA**. The **IL** units modified on the electrode are expected to prevent dye aggregation. Their cationic character may be advantageous for the smooth transport of the anionic redox couple (I₃[–]/I[–]). In this study, we prepared **IL**-modified TiO₂ electrodes encapsulating the sensitising dyes **N3** and **J13**. **N3** is a dye with high photovoltaic performance,³ and **J13**³¹ is one of the ruthenium complex-based dyes in the **J** series that was previously synthesised by our group.^{32–34} We fabricated DSSCs using these dyes with **IL**-modified TiO₂ electrodes and evaluated their photovoltaic performances. DSSCs using **IL**-modified TiO₂ electrodes showed higher anti-aggregation effect than those using the conventional anti-aggregation agent, **CDCA**.

Experimental

General

¹H NMR spectra were recorded on a Varian Gemini-2000 XL-300 MHz FT NMR spectrometer with TMS as the internal standard. Electronic absorption (UV/vis) spectra were recorded using

a JASCO V-570 UV/vis spectrophotometer. Infrared (IR) spectra were recorded using a JASCO FT/IR-4200 spectrometer. Electrospray ionisation mass spectra (ESI-MS) were obtained with a Micromass LCT ESI-TOF MS. Wavelength-dispersive X-ray spectroscopy (WDS) measurements were recorded using JEOL electron probe microanalysers JXA-8230 and JXA-8530F. Elemental analysis was performed using an Elemental Vario El Cube CHNOS analyser.

Chemicals

All reagents and organic solvents were purchased from Kanto Chemical, Kishida Chemical, Nacalai Tesque, Sigma-Aldrich, TCI, Wako Pure Chemical Industries, and Yoneyama Yakuhin Kogyo, and were used without further purification. Distilled water was obtained from an EYELA SA-2100E automatic water distillation apparatus. Thin-layer chromatography (TLC) was performed using a Merck TLC Silica 60 F254. Column chromatography was carried out with Kanto Chemical spherical silica gel 60 N (neutral, 63–210 µm).

Solar cell fabrication

A Pilkington fluorine doped tin oxide (FTO) glass plate (Tec15, ohm per sq) was cut into a 2 × 2 cm piece and washed in MeCN for 30 min using an ultrasonic cleaning machine. The TiO₂ paste (PST-18NR) was deposited on the FTO glass plate (as an adsorption layer for the dye chromophore) and heated at 100 °C for 10 min. The electrode was coated with TiO₂ paste (PST-400C) as a light-scattering layer, and sintered at 530 °C for 1 h. After cooling, the TiO₂/FTO electrode was immersed in a *tert*-butyl alcohol/MeCN (1 : 1, v/v) solution containing 0.3 mM of sensitised dye (**N3** or **J13**) and various concentrations of ionic liquid (**IL**₆₆₆₄ or **IL**₆₆₆₁₁) for half a day. After washing with the *tert*-butyl alcohol/MeCN solution, the resultant dye/**IL**-modified TiO₂/FTO electrode was used as the electrode of the DSSC. Reference cells were prepared by immersing the plate in a 0.3 mM *tert*-butyl alcohol/MeCN (1 : 1, v/v) solution containing **N3** or **J13** for half a day. To prepare the platinum electrode, an FTO plate was dipped into a 30 mM solution of 2-propanol and H₂PtCl₆·6H₂O, then burnt at 385 °C for 30 min. The Pt electrode and TiO₂/FTO

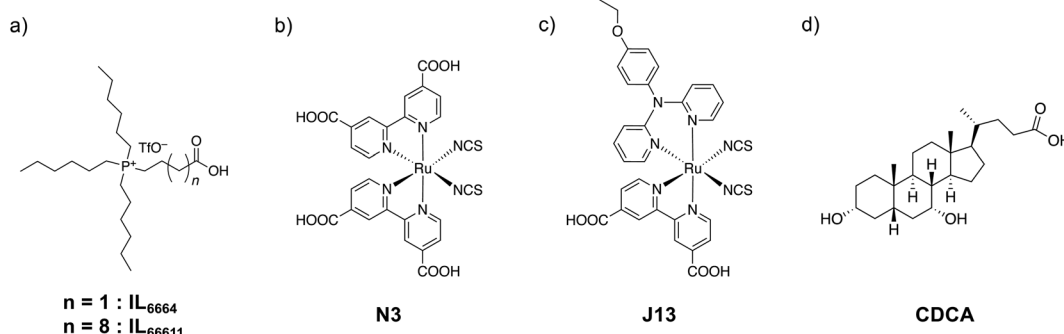


Fig. 1 Schematic views of (a) ionic liquids used for the surface modification of electrodes (IL_{6664} and IL_{66611}). (b) **N3** dye, (c) **J13** dye, and (d) chenodeoxycholic acid (**CDCA**).



electrodes covered with dye or dye/IL were pasted using epoxy-based adhesive or UV-cured resin. An electrolyte comprising LiI (0.1 M), I₂ (0.05 M), 1,2-dimethyl-3-propylimidazolium iodide (0.6 M), and 4-*tert*-butylpyridine (0.5 M) in MeCN (HPLC grade) was used.

Estimation of surface coverage of adsorbed dyes and ILs on TiO₂ electrodes

The amounts of N3 and J13 adsorbed were estimated using UV/vis spectroscopy after base treatment. A 0.1 M NaOH solution (for N3) and a 0.1 M NaOH solution in H₂O/MeOH (1 : 1) (for J13) were used for the base treatments. WDS measurements were recorded to determine the surface ratios of the dyes and ILs. The surface coverages of the ILs were estimated from the ratio of P atoms (originating from ILs) to Ru atoms (originating from the dyes).

Photovoltaic measurements

The photovoltaic performance of the DSSCs was measured with an Asahi Spectra IVP-0605 current–voltage (*I*–*V*) curve measurement recorder. An Asahi Spectra HAL-302 solar simulator was used to simulate the intensity of 1 sun (100 mW cm^{−2}, AM 1.5) at the surface of the DSSC samples. To ensure that the irradiation area is identical across all samples, each DSSC was covered with a black tape containing a hole (size: 0.07 cm²) during the measurements to minimise the influence of stray light. Incident photo-to-current conversion efficiency (IPCE) spectra for DSSCs based on N3/TiO₂ and N3 + IL₆₆₆₁₁/TiO₂ were recorded with a Newport benchtop optical power meter model 1936-R using an Asahi Spectra PVL-4000 EX3 wavelength-tunable light source.

EIS spectra measurements

The EIS spectra of N3/TiO₂ and N3 + IL₆₆₆₁₁/TiO₂ were carried out using an ALS/CH Instruments electrochemical analyzer model 660EKA. EIS measurements were performed at several potentials of the substrates with a frequency range from 10^{−2} to 10⁶ Hz at an amplitude of 5 mV.

Preparation of ILs and Ru complex dyes

The ILs (IL₆₆₆₄ and IL₆₆₆₁₁) were prepared according to Scheme S1† and the procedures are described below. The ¹H NMR, FT-IR, and ESI-TOF MS spectra of the ILs are shown in Fig. S1–S6.† The Ru complex dyes, N3 and J13, were prepared according to previous methods.^{3,31} The ESI-TOF MS and ¹H NMR spectra of the N3 and J13 are shown in Fig. S7–S9.†

Synthesis of 4-(carboxypropyl)triethylphosphonium bromide. 4-Bromobutyric acid (36.5 mmol) was dissolved in toluene (60 mL) under Ar in a 300 mL eggplant flask. A solution containing toluene (120 mL) and triethylphosphine (36.5 mmol) was then added dropwise to the flask over 6 h. The resultant solution was stirred for one week under Ar atmosphere at room temperature. The solution was then evaporated using a vacuum line, giving a viscous liquid. After washing with hexane, the liquid was purified using column chromatography

(CHCl₃/MeOH, 11 : 1), giving a colourless viscous liquid. Yield: 2.50 g (15%).

Synthesis of 4-(carboxypropyl)triethylphosphonium trifluoro-methanesulfonate (IL₆₆₆₄). 4-(Carboxypropyl)triethylphosphonium bromide (7.67 mmol) was dissolved in THF (10 mL) in a 100 mL eggplant flask. A solution containing THF (5 mL) and trifluoromethanesulfonate (11.35 mmol) was added to the flask, and the mixture was stirred for 1 h at room temperature. The solution was filtered using Celite, and the filtrate was evaporated using a vacuum line. The residue was dissolved in CH₂Cl₂ (50 mL) and washed thrice with Milli-Q water (50 mL). Residual Cl[−] ions were removed by adding aqueous AgNO₃ into the aqueous layer. The organic layer was dried using anhydrous Na₂SO₄. After evaporation *in vacuo*, a yellow viscous liquid was obtained. The liquid was purified using column chromatography (CHCl₃/MeOH, 11 : 1). Yield: 1.56 g (39%). ¹H NMR (CD₃OD, 300 MHz) δ ppm: 0.95 (t, 9H, −CH₃), 1.31–1.63 (m, 24H, −CH₂−), 1.88 (m, 2H, −CH₂−), 2.23–2.35 (m, 8H, P⁺CH₂−), 2.55 (t, 2H, −CH₂COOH). FT-IR (DR, cm^{−1}): 2934 (ν_{C–H}), 1732 (ν_{C=O}), 1256 (ν_{SO₃[−]}), 1222 (ν_{C–F}), 1156 (ν_{C–F}), 1031 (ν_{SO₃[−]}). ESI TOF-MS (positive mode) *m/z* = 373.42 ([M]⁺).

Synthesis of 11-(carboxypropyl)triethylphosphonium bromide. 11-(Carboxypropyl)triethylphosphonium bromide was synthesised in the same manner as 4-(carboxypropyl)-triethyl-phosphonium bromide. 11-Bromoundecanoic acid was used instead of 4-bromobutyric acid. Yield: 1.00 g (10%).

Synthesis of 11-(carboxypropyl)triethylphosphonium trifluoromethanesulfonate (IL₆₆₆₁₁). IL₆₆₆₁₁ was synthesised in the same manner as IL₆₆₆₄. 11-(Carboxypropyl)triethylphosphonium bromide (1.52 mmol) was used instead of 4-(carboxypropyl)-triethylphosphonium bromide. Yield: 113.3 mg (49%). ¹H NMR (CDCl₃, 300 MHz) δ ppm: 0.94 (t, 9H, −CH₃), 1.27–1.58 (m, 40H, −CH₂−), 2.16–2.30 (m, 10H, P⁺CH₂−, −CH₂COOH). FT-IR (DR, cm^{−1}): 2933 (ν_{C–H}), 1732 (ν_{C=O}), 1257 (ν_{SO₃[−]}), 1223 (ν_{C–F}), 1157 (ν_{C–F}), 1030 (ν_{SO₃[−]}). ESI TOF-MS (positive mode) *m/z* = 471.43 ([M]⁺).

Results and discussion

Preparation of ILs and sensitised Ru complex dyes

For the modification of ILs on the TiO₂ electrode surface, tertiary phosphonium-type ILs with terminal carboxylic acids were synthesised. The terminal carboxylic acid is well known as the anchor group for the modification of the TiO₂ electrode surface.²⁰ The carboxylic acid and −OH groups on the TiO₂ surface are condensed *via* dehydrogenation. As a result, molecules containing carboxyl groups are strongly bonded to the TiO₂ surface. ILs with different alkyl chain lengths (Fig. 1a) were designed and synthesised to evaluate the effects of ILs on the photovoltaic performance of DSSCs. The numerical abbreviations of the ILs (IL₆₆₆₄ and IL₆₆₆₁₁) refer to the number of C atoms in each alkyl moiety (the linker moiety contains the C atom of the carboxyl group). The ILs were prepared based on our previous reports on ILs with disulfide groups for Au surface modification.²⁷ All ILs were synthesised by reacting triethylphosphine with carboxylic acids containing a terminal bromide group. IL₆₆₆₄ was obtained as a solid, likely because of



Table 1 Adsorption amounts of N3 and ILs (IL_{6664} and IL_{66611}) under various immersion conditions

TiO ₂ electrode	Immersion condition (N3 dye : IL)	Ratio of N3 dye : IL on TiO ₂	Amount of N3 dye adsorbed on TiO ₂ (mol cm ⁻²)	N3 dye decrease rate (%)	Amount of IL adsorbed on TiO ₂ (mol cm ⁻²)
N3/TiO ₂	—	—	8.73×10^{-8}	—	—
N3 + IL_{6664} /TiO ₂	1 : 5	1 : 0.68	6.42×10^{-8}	23	4.37×10^{-8}
	1 : 10	1 : 0.85	5.95×10^{-8}	32	5.06×10^{-8}
	1 : 15	1 : 0.87	5.64×10^{-8}	35	4.91×10^{-8}
N3 + IL_{66611} /TiO ₂	1 : 1	1 : 0.18	7.95×10^{-8}	8.9	1.43×10^{-8}
	1 : 10	1 : 0.47	8.12×10^{-8}	7.0	3.83×10^{-8}
	1 : 20	1 : 0.59	8.18×10^{-8}	6.3	4.83×10^{-8}
	1 : 50	1 : 0.78	8.03×10^{-8}	8.0	6.26×10^{-8}
	1 : 100	1 : 1.00	8.32×10^{-8}	4.7	8.32×10^{-8}

its short alkyl chains. IL_{66611} was obtained as a viscous liquid owing to its long alkyl chains. The ILs were characterised by ¹H NMR, FT-IR, and ESI-MS spectroscopy.

N3 and J13 were chosen as the sensitising dyes in this study. The structures of the dyes are shown in Fig. 1b. N719 is often used as the standard dye in studies involving DSSCs. However, N719 contains two tetrabutylammonium ion (TBA^+) units, which are introduced through a cation exchange reaction of N3. In this study, we used quaternary phosphonium-type ILs, which are very similar to quaternary ammonium cations, such as the TBA^+ units in N719. Therefore, when N719 will be used in this study, an unfavourable cation exchange reaction will occur between TBA^+ and the ILs. To exclude the cation exchange effect and evaluate the net effect of ILs, we decided to use the N3 dye in this study. The J13 dye, which we previously developed, has a relatively high conversion efficiency.³¹ In this study, N3 and J13 were used to study the effects for dye materials with different structures. Furthermore, the I^-/I_3^- redox couple was used for all DSSCs fabricated in this study. Our previous studies using ILs-modified substrates indicate that the relatively large-sized molecules are blocked their transportation between the modified ILs layer on the electrode and the electrolyte solution interface.²⁷⁻²⁹ Thus, we chose the I^-/I_3^- redox couple as the small and typical one for the DSSCs in this study. The dyes were synthesised according to a previously reported method and were characterised by ¹H NMR, ESI-MS, FT-IR, UV/vis spectroscopy, and elemental analysis.

Preparation of IL- and N3-modified TiO₂ electrodes

The modification of ILs and N3 onto the TiO₂ surfaces was carried out by immersing the TiO₂ electrodes in a solution of *tert*-butyl alcohol/acetonitrile (1 : 1) containing the ILs and N3. Table 1 lists the adsorption values of the ILs and N3. Solutions containing N3 and ILs of different alkyl chain lengths (IL_{6664} and IL_{66611}) at various concentrations were prepared and the TiO₂ electrodes were immersed in them. The concentration of N3 was fixed at 0.3 mM, and the concentration of ILs was varied in the range of 1–100 equivalents to N3. The amount of N3 adsorbed on the surface was estimated using the UV/vis spectra recorded after desorption from the TiO₂ surface by treatment with a base. The ratio of N3 to ILs adsorbed was estimated using the WDS measurements of Ru atoms from N3 and P atoms from the ILs.

As the ratio of IL_{6664} to N3 on the TiO₂ electrode increased, the amount of N3 adsorbed decreased significantly, whereas the amount of IL_{6664} adsorbed did not change significantly (only N3 adsorption decreased by 35% at $\text{IL}_{6664} : \text{N3} = 1 : 0.87$). There was no significant difference in the adsorption rate of N3 to IL_{6664} on the TiO₂ surface. Therefore, we postulated that the adsorption of N3 was hindered to some extent when IL_{6664} was adsorbed on the surface. In our previous study, we reported that bulky ILs modified with thiol groups on Au electrodes can create adequate space between ILs for relatively large molecules to be introduced into them.²⁷⁻²⁹ As seen in Fig. 1a, the $-\text{CH}_2-$ linker chain in IL_{6664} is very short. When IL_{6664} is modified, there is not enough space between the modified ILs on TiO₂ to adsorb the N3 dye; thus, the surface coverage of N3 decreases.

In contrast, for IL_{66611} , which has a long $-\text{CH}_2-$ linker chain, there was no significant decrease in the amount of N3 adsorbed, even when the ratio of IL in the soaking solution increased (the maximum decrease in the amount of N3 adsorbed was less than 10%). The amount of IL_{66611} adsorbed increased as the ratio of IL in the soaking solution increased. This indicates that N3 is first adsorbed on TiO₂, followed by IL_{66611} , which is adsorbed in the gaps between the adsorbed N3 particles. Due to the long $-\text{CH}_2-$ chain in IL_{66611} (Fig. 1a), the adsorption of IL_{66611} was not inhibited by the adsorption of N3 on the exposed TiO₂ surface. Because all the ILs had the same headgroup (triethylphosphonium moiety), it was suggested that the size of the space created on TiO₂ depends on the length of the $-\text{CH}_2-$ linker chain, which had a significant effect on the adsorption surface area of N3.

Photovoltaic performance of DSSCs with IL-modified TiO₂ electrodes

Based on the surface coverages of N3 and ILs on TiO₂, IL_{66611} was found to be a suitable candidate as an anti-aggregation agent. Thus, we evaluated the photovoltaic performance of DSSCs using IL_{66611} . Fig. 2 shows the *I*-*V* characteristics of the DSSCs with N3/TiO₂ and N3 + IL_{66611} /TiO₂ electrodes. The photovoltaic parameters are listed in Table 2. The open-circuit voltage (V_{oc}), short-circuit current density (J_{sc}), fill factor (FF), and conversion efficiency (η) of the N3-based DSSC are 0.590 V, 13.9 mA cm⁻², 0.673, and 5.54%, respectively. The introduction of IL_{66611} improved all the photovoltaic parameters of the DSSCs



with **N3** + **IL**₆₆₆₁₁/TiO₂ electrodes. In particular, the greatest improvement in efficiency was observed for the electrode modified with **N3** and **IL**₆₆₆₁₁ in the ratio of 1 : 1. The V_{OC} , J_{SC} , FF, and η of the DSSC are 0.641 V, 15.9 mA cm⁻², 0.705, and 7.20%, respectively. This shows a 30% increase in efficiency compared to that of **N3** only. Although the surface coverage of **N3** adsorbed on TiO₂ was slightly decreased by **IL** modification, all the photovoltaic parameters of the DSSCs improved. This suggests that the modification with **ILs** achieved an anti-aggregation effect and suppressed reverse electron transfer. The reduction of dark current (Fig. 2b) suggests that **ILs** suppress the direct electron transfer between the TiO₂ electrode and the I⁻/I₃⁻ redox couple. Fig. S10[†] shows the IPCE spectra of the DSSCs based on **N3**/TiO₂ and **N3** + **IL**₆₆₆₁₁/TiO₂ (1 : 0.78 and 1 : 1.00). The IPCE values of two DSSCs based on **N3** + **IL**₆₆₆₁₁/TiO₂ were improved than that of **N3**/TiO₂ in all measurement regions. This phenomenon also indicates that the **IL**₆₆₆₁₂ units modified on the TiO₂ electrode surface work as a good anti-aggregation reagent.

The performances of the solar cells with the **J13** dye are shown in Fig. 3 and Table 3. The V_{OC} , J_{SC} , FF, and η of the DSSC with only **J13** are 0.574 V, 10.2 mA cm⁻², 0.612, and 3.58%, respectively. Similarly, as in the case of **N3**, the introduction of **ILs** greatly improved the photovoltaic parameters. The most significant improvement was observed for the electrode modified by **J13** and **IL**₆₆₆₁₁ at a 1 : 0.29 ratio, where V_{OC} , J_{SC} , FF, and η are 0.641 V, 11.6 mA cm⁻², 0.648, and 4.80%, respectively. In this case, the conversion efficiency of the DSSC fabricated with **J13** + **IL**₆₆₆₁₁/TiO₂ was 34% higher than that of the DSSC fabricated with **J13** only. The same effect was observed for different dyes, suggesting that the modification with **ILs** is very effective in inhibiting dye aggregation and reverse electron transfer. As in the case of **N3**, the dark current of **J13** was also reduced upon modification with **ILs** (Fig. 2b). For both **N3** and **J13**, the effect of **IL**₆₆₆₁₁ modification was significant. However, despite similar immersion conditions, the amount of **IL**₆₆₆₁₁ adsorbed on the TiO₂ electrode with **J13** was lower than that with **N3** (Tables 2 and 3). This could be due to differences in the adsorption structures of the dyes on the TiO₂ surface. The **N3** dye had four carboxyl groups, whereas the **J13** dye had only two carboxyl

groups, as well as a terminal C₄H₉O⁻ group. Thus, the orientation of **J13** on the TiO₂ surface is more suppressed than that of **N3**. These structural characteristics probably caused steric hindrance with the **ILs**. As a result, the unmodified area of the TiO₂ surface of the DSSC with **J13** + **IL**₆₆₆₁₁ appeared to be larger than that of the DSSC with **N3** + **IL**₆₆₆₁₁.

Performance of **ILs** as anti-aggregation agents

The performance of **IL**₆₆₆₁₁ as an anti-aggregation agent was compared to that of solar cells fabricated using and chenodeoxycholic acid (**CDCA**), a conventional anti-aggregation agent. The results are summarised in Table 4. The performance of the solar cells with **N3** decreased with the introduction of **CDCA**, which could be due to the decrease in the surface coverage of **N3** (the surface coverage of **N3** decreased to approximately 30% upon modification with **CDCA**). In contrast, the performance of the solar cells with **IL**₆₆₆₁₁ improved significantly. When **IL**₆₆₆₁₁ was used, the decrease in surface coverage of **N3** was considerably lower (the **N3** coverage only decreased to approximately 95%). This could be because **IL**₆₆₆₁₁ was able to enter the interstitial space of the **N3** dye, preventing aggregation without reducing the amount of **N3** adsorbed. When the same experiment was carried out with **J13**, the results were very similar to those of **N3**. This is because **IL**₆₆₆₁₁ can be adsorbed onto the surface without reducing the amount of dye adsorbed, as explained above. In other words, **IL**₆₆₆₁₁ can act as an anti-aggregation agent for various sensitising dyes. In addition, unlike **CDCA**, **IL**₆₆₆₁₁ has a positive charge, which may improve the conversion efficiency. To clarify the role of the **ILs** modified on the TiO₂ surface, we measured the EIS spectra of **N3**/TiO₂ and **IL**₆₆₆₁₁/TiO₂ in the electrolyte solution. EIS spectra are often used to analyse the various interfaces on the electrodes.^{35,36} The results of the measurements of the EIS spectra at different potentials are shown in Fig. S11 and S12.[†] The several parameters related to the surface resistances and capacitances summarized in the figures were obtained by the curve-fitting of the Nyquist plots of **N3**/TiO₂ and **N3** + **IL**₆₆₆₁₁/TiO₂ using the equivalent circuit shown in Fig. S13.[†] The surface-modified **ILs** did not affect the R_{ct1} values which are the resistances between

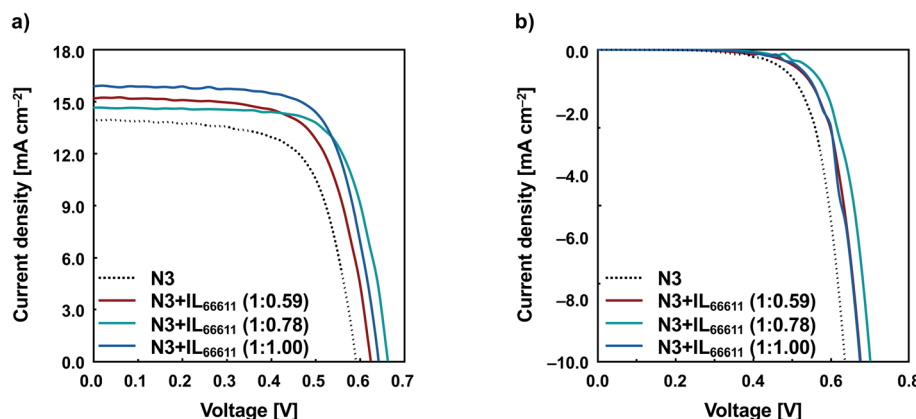
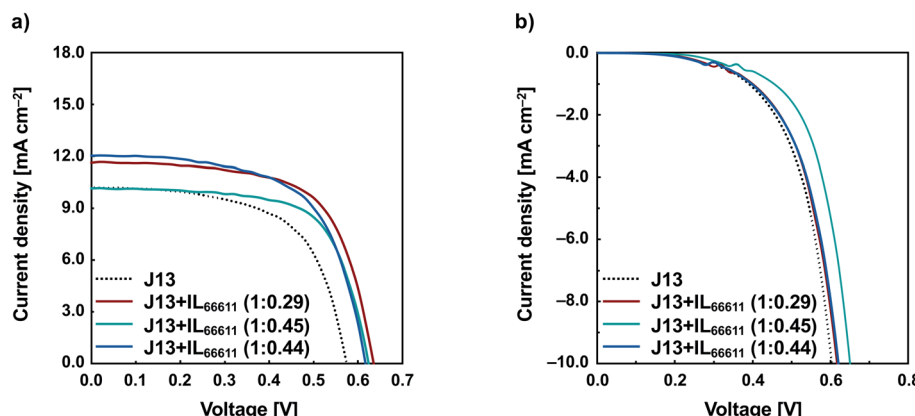


Fig. 2 Current–voltage characteristics of DSSCs with **N3** and **N3** + **IL**₆₆₆₁₁ (a) under irradiation and (b) in the dark.



Table 2 Photovoltaic performance of DSSCs with N3 and N3 + IL₆₆₆₁₁

DSSC	Immersion condition (N3 dye : IL)	Ratio of N3 dye : IL on TiO ₂	V _{OC} (V)	J _{SC} (mA cm ⁻²)	FF	η (%)	Increase rate of η (%)
N3	—	—	0.590	13.9	0.673	5.54	—
N3 + IL₆₆₆₁₁/TiO₂	1 : 20	1 : 0.59	0.593	15.2	0.682	6.47	17
	1 : 50	1 : 0.78	0.663	14.7	0.715	6.95	25
	1 : 100	1 : 1.00	0.641	15.9	0.705	7.20	30

Fig. 3 Current–voltage characteristics of DSSCs with J13 and J13 + IL₆₆₆₁₁ (a) under irradiation and (b) in the dark.Table 3 Photovoltaic performance of DSSCs with J13 and J13 + IL₆₆₆₁₁

DSSC	Immersion condition (J13 dye : IL)	Ratio of J13 dye : IL on TiO ₂	V _{OC} (V)	J _{SC} (mA cm ⁻²)	FF	η (%)	Increase rate of η (%)
J13	—	—	0.574	10.2	0.612	3.58	—
J13 + IL₆₆₆₁₁/TiO₂	1 : 20	1 : 0.29	0.641	11.6	0.648	4.80	34
	1 : 50	1 : 0.45	0.614	10.2	0.671	4.22	18
	1 : 100	1 : 1.44	0.617	12.0	0.622	4.62	29

Table 4 Comparison of CDCA and IL₆₆₆₁₁ as the anti-aggregation agent for DSSCs

DSSC	V _{OC} (V)	J _{SC} (mA cm ⁻²)	FF	η (%)	Increase rate of η (%)
N3	0.590	13.9	0.673	5.54	—
N3 + CDCA/TiO₂	0.633	10.0	0.679	4.30	-22
N3 + IL₆₆₆₁₁/TiO₂	0.641	15.9	0.705	7.20	+30
J13	0.574	10.2	0.612	3.58	—
J13 + CDCA/TiO₂	0.578	8.78	0.627	3.18	-11
J13 + IL₆₆₆₁₁/TiO₂	0.641	11.6	0.648	4.62	+34

the FTO and the TiO₂ electrodes. On the other hand, the R_{ct2} values which are the resistances between the TiO₂ surface and the electrolyte solution were lowered by the ILs on the TiO₂ surfaces. These phenomena indicate that the positively-charged ILs on the TiO₂ surface contribute to the decline of the interface resistance between the TiO₂ surface and the electrolyte solution.

Furthermore, it is known that the introduction of a cation (such as TBA⁺) into some of the carboxylic acid moieties of N3 improves solar cell performance. From the DFT calculations, it

was found that this was due to the increase in the energy level of N719 when the carboxylic acid moiety was replaced with TBA⁺.⁵ In this study, one of the possible reasons for the improved solar cell performance is also that the positive charge of the ILs has the same effect as TBA⁺ and interacted with the carboxylic acid moieties that were not adsorbed.

From our previous studies, the IL-modified substrates have enhanced the stability and durability of the entrapped compounds.^{28,29} The IL-modified TiO₂ electrodes are expected to



have a similar effect on the surface-modified dyes. However, due to factors such as the durability of the fabricated DSSC (e.g., electrolyte leakage) for long-time measurements, it is currently not achieved to evaluate the effect of the IL units modified on the TiO_2 electrode. Now, we are attempting to rigorously evaluate the contribution of the IL-modified electrodes to the durability of DSSCs.

Conclusions

Ionic liquid-modified TiO_2 electrodes were used to prevent the aggregation of dyes on the electrodes and improve the photovoltaic performance of DSSCs. The structures of the dyes and ILs had a significant effect on the surface coverage of the dyes adsorbed on the TiO_2 surface. Using IL₆₆₆₁₁ with a long $-\text{CH}_2-$ linker chain, we succeeded in reducing the decrease in the amount of dye adsorbed. ILs were also found to outperform the conventional anti-aggregation agent, CDCA. It was shown that the use of positively-charged ILs as anti-aggregation agents enhanced the performance of solar cells without reducing the amount of dye adsorbed. The advantage of the ILs used in this study is that various structures can be synthetically designed, and we believe that they can be used as new anti-aggregation agents in the future.

Author contributions

Conceptualization, T. I. and H. M.; methodology, T. I., A. M., G. J., and T. K.; validation, T. I. and T. O.; formal analysis, A. M., G. J., T. K., and M. M.; investigation, A. M., G. J., and A. M.; data curation, T. I., A. M., G. J. and M. M.; writing—original draft preparation, T. I.; writing—review and editing, T. I. and H. M.; visualization, T. I.; supervision, T. I. and T. O.; project administration, T. I. and H. M.; funding acquisition, T. I. and H. M. All authors have read and agreed to the published version of the manuscript.

Conflicts of interest

There are no conflicts to declare.

Acknowledgements

This work was supported in part by a Grant-in-Aid for Scientific Research from the Ministry of Culture, Sports, Science, and Technology, Japan (MEXT/JSPS KAKENHI Grant Number (B) 20H02752 and (C) 21K04664 for H. M. and T. I., respectively). This study was also supported by the Murata Science Foundation. We would like to express our gratitude to them.

Notes and references

- 1 K. Kalyanasundaram, *Dye-sensitized solar cells*, EPFL Press, Lausanne, 2010.
- 2 *Dye-Sensitized Solar Cells: Mathematical Modelling, and Materials Design and Optimization*, ed. M. Soroush and K. K. S. Lau, 2019.

- 3 M. K. Nazeeruddin, A. Kay, I. Rodicio, R. Humphry-Baker, E. Mueller, P. Liska, N. Vlachopoulos and M. Grätzel, *J. Am. Chem. Soc.*, 1993, **115**, 6382–6390.
- 4 M. K. Nazeeruddin, S. M. Zakeeruddin, R. Humphry-Baker, M. Jirousek, P. Liska, N. Vlachopoulos, V. Shklover, C.-H. Fischer and M. Grätzel, *Inorg. Chem.*, 1999, **38**, 6298–6305.
- 5 M. K. Nazeeruddin, F. De Angelis, S. Fantacci, A. Selloni, G. Viscardi, P. Liska, S. Ito, B. Takeru and M. Grätzel, *J. Am. Chem. Soc.*, 2005, **127**, 16835–16847.
- 6 A. Yella, H. W. Lee, H. N. Tsao, C. Yi, A. K. Chandiran, M. K. Nazeeruddin, E. W. Diau, C. Y. Yeh, S. M. Zakeeruddin and M. Grätzel, *Science*, 2011, **334**, 629–634.
- 7 P. Wang, S. M. Zakeeruddin, R. Humphry-Baker, J. E. Moser and M. Grätzel, *Adv. Mater.*, 2003, **15**, 2101–2104.
- 8 P. Wang, S. M. Zakeeruddin, P. Comte, R. Charvet, R. Humphry-Baker and M. Grätzel, *J. Phys. Chem. B*, 2003, **107**, 14336–14341.
- 9 P. Wang, S. M. Zakeeruddin, R. Humphry-Baker and M. Grätzel, *Chem. Mater.*, 2004, **16**, 2694–2696.
- 10 A. Kay and M. Graetzel, *J. Phys. Chem.*, 1993, **97**, 6272–6277.
- 11 Z.-S. Wang, Y. Cui, Y. Dan-oh, C. Kasada, A. Shinpo and K. Hara, *J. Phys. Chem. C*, 2007, **111**, 7224–7230.
- 12 N. R. Neale, N. Kopidakis, J. van de Lagemaat, M. Gratzel and A. J. Frank, *J. Phys. Chem. B*, 2005, **109**, 23183–23189.
- 13 S. Qu, W. Wu, J. Hua, C. Kong, Y. Long and H. Tian, *J. Phys. Chem. C*, 2009, **114**, 1343–1349.
- 14 H. Matsuzaki, T. N. Murakami, N. Masaki, A. Furube, M. Kimura and S. Mori, *J. Phys. Chem. C*, 2014, **118**, 17205–17212.
- 15 P. J. Cameron and L. M. Peter, *J. Phys. Chem. B*, 2003, **107**, 14394–14400.
- 16 M. S. Góes, E. Joanni, E. C. Muniz, R. Savu, T. R. Habeck, P. R. Bueno and F. Fabregat-Santiago, *J. Phys. Chem. C*, 2012, **116**, 12415–12421.
- 17 P. Lellig, M. A. Niedermeier, M. Rawolle, M. Meister, F. Laquai, P. Muller-Buschbaum and J. S. Gutmann, *Phys. Chem. Chem. Phys.*, 2012, **14**, 1607–1613.
- 18 E. Palomares, J. N. Clifford, S. A. Haque, T. Lutz and J. R. Durrant, *J. Am. Chem. Soc.*, 2003, **125**, 475–482.
- 19 M. Cai, X. Pan, W. Liu, J. Bell and S. Dai, *RSC Adv.*, 2015, **5**, 33855–33862.
- 20 D. Song, H. An, J. H. Lee, J. Lee, H. Choi, I. S. Park, J. M. Kim and Y. S. Kang, *ACS Appl. Mater. Interfaces*, 2014, **6**, 12422–12428.
- 21 *Ionic liquids IV: not just solvents anymore*, ed. J. F. Brennecke, R. D. Rogers and K. R. Seddon, American Chemical Society, Washington, 2008.
- 22 *Ionic liquids for better separation processes*, ed. H. Rodríguez, Springer, 2016.
- 23 S. Y. Lee, A. Ogawa, M. Kanno, H. Nakamoto, T. Yasuda and M. Watanabe, *J. Am. Chem. Soc.*, 2010, **132**, 9764–9773.
- 24 G. P. Lau, H. N. Tsao, S. M. Zakeeruddin, M. Grätzel and P. J. Dyson, *ACS Appl. Mater. Interfaces*, 2014, **6**, 13571–13577.
- 25 T. C. Chu, R. Y. Lin, C. P. Lee, C. Y. Hsu, P. C. Shih, R. Lin, S. R. Li, S. S. Sun, J. T. Lin, R. Vittal and K. C. Ho, *ChemSusChem*, 2014, **7**, 146–153.



26 H. Sakaue and H. Matsumoto, *Electrochem. Commun.*, 2003, 5, 594–598.

27 T. Kitagawa, T. Inomata, Y. Funahashi, T. Ozawa and H. Masuda, *Chem. Commun.*, 2013, **49**, 10184–10186.

28 T. Kitagawa, J. Nishino, T. Inomata, T. Ozawa, Y. Funahashi and H. Masuda, *Chem. Commun.*, 2016, **52**, 4780–4783.

29 T. Kitagawa, T. Yano, T. Inomata, T. Ozawa and H. Masuda, *Chem. Lett.*, 2016, **45**, 436–438.

30 G. Iijima, T. Kitagawa, A. Katayama, T. Inomata, H. Yamaguchi, K. Suzuki, K. Hirata, Y. Hijikata, M. Ito and H. Masuda, *ACS Catal.*, 2018, **8**, 1990–2000.

31 Z. Jin, H. Masuda, N. Yamanaka, M. Minami, T. Nakamura and Y. Nishikitani, *J. Phys. Chem. C*, 2009, **113**, 2618–2623.

32 Z. Jin, H. Masuda, N. Yamanaka, M. Minami, T. Nakamura and Y. Nishikitani, *ECS Trans.*, 2008, **16**, 61–70.

33 Z. Jin, H. Masuda, N. Yamanaka, M. Minami, T. Nakamura and Y. Nishikitani, *ChemSusChem*, 2008, **1**, 901–904.

34 Z. Jin, H. Masuda, N. Yamanaka, M. Minami, T. Nakamura and Y. Nishikitani, *Chem. Lett.*, 2009, **38**, 44–45.

35 F. Fabregat-Santiago, G. Garcia-Belmonte, I. Mora-Sero and J. Bisquert, *Phys. Chem. Chem. Phys.*, 2011, **13**, 9083–9118.

36 A. R. C. Bredar, A. L. Chown, A. R. Burton and B. H. Farnum, *ACS Appl. Energy Mater.*, 2020, **3**, 66–98.

